

NATIONAL TRANSPORTATION SAFETY BOARD

Office of Research and Engineering
Materials Laboratory Division
Washington, D.C. 20594



October 2, 2001

MATERIALS LABORATORY FACTUAL REPORT

Report No. 01-120

A. ACCIDENT

Place : Near Port Hueneme, California
Date : January 31, 2000
Vehicle : Boeing MD-83, N963AS
Operator : Alaska Airlines, Flight 261
NTSB No. : DCA00-M-A023

B. COMPONENTS EXAMINED

Fractographic Specimens from a new torque tube and one removed from N982AS.
Torque Tube fractures from Quill Shaft Tests I and II.

C. DETAILS OF THE EXAMINATION

On October 5, 2000 a series of tests were undertaken to produce low cycle fatigue (LCF) fractures in threaded specimens of jackscrew assembly torque tube material, p/n 5914170-1. The produced fracture features were examined for comparison to the fractured accident torque tube documented in Metallurgical Factual Report 00-145.

Additionally, the torque tubes fractured during Quill Shaft Tests (QST) I and II¹ were fractographically examined.

Most tests and examinations were performed at the Boeing M&PE Laboratory in Huntington Beach, California under the control and supervision of the Metallurgy Group.

Specimens

To perform the test a total of five standard configuration ASTM E-8 0.5-inch nominal diameter tensile specimens were machined from the new torque tube used in QST I and from the original torque tube installed in jackscrew assembly DCA3000 removed from aircraft N982AS². Figure 1 shows the pieces of torque tube from which the specimens were removed.

¹ Quill Shaft Test I was performed on July 26, 2000. Quill Shaft Test II was performed on October 2, 2000. Both are documented in the Aircraft Structures Group Report.

² Documented in Metallurgical Factual Report 00-146.

The standard tensile test specimens were modified by machining partial thread profiles into the central portion of the gage length of each specimen. The threads cut into the tensile bars had modified profiles based on 1/2-20UNF-3A threads³. However, the maximum depth of the threads approximately 0.025-inch and the thread roots were filleted. At least four full threads were present between starter threads. Following the tests, the thread root radii on all specimens were measured using an optical comparator. The measurements averaged 0.0085 inch. Figure 2 displays the specimens and a close up view of a typical threaded area.

Material

The p/n 5914170-1 torque tubes used for the test specimens were manufactured from Ti-6Al-4V titanium alloy forgings, per Douglas Material Specification DMS 1583 and forged per DMS 1881, Class 2. The drawing specifies a minimum 140,000 psi minimum ultimate strength. The chemistry and tensile properties of the new torque tube used in QST I were determined to be in compliance with the applicable specifications⁴. The chemical composition of the torque tube from N982AS was also determined to be in compliance with applicable specifications.

Procedure

The first test specimen, N-3A, was used to set up the test apparatus and was cycled at several different stress levels to establish parameters for the additional test. This sample also utilized a 10° angle washer under one end in an attempt to produce off-axis loading of the sample. However the use of an angle washer was discontinued because it produced unwanted bending loads and physically bent the specimen at one end, see figure 3. All remaining tests were operated under straight tension- tension conditions.

Three test specimens, N-1B, N-1A and N-2A, were cyclically loaded at various stress ranges in a computer controlled tensile test apparatus. The loads were applied at constant amplitude using a stress ratio⁵ (R) of 0.1 and a loading frequency of 1 Hertz (1 cycle per second). The maximum stresses applied to the three specimens (N-1B, N-1A and N-2A) were arbitrarily chosen to be approximately 140,000 psi, 165,000 psi and 185,000 psi based on the minor diameter of the threaded section of the specimen. Each specimen was cycled at constant rates and stresses until fracture and the number of cycles and load at fracture were recorded.

³ The threads on torque tubes are specified as 7/8-14 UNF-3A per MIL-S-7742 that in turn specifies either Mil-S-8879 or FED-STD-H28/2 for dimensions.

⁴ The new torque tube used in QST I and for specimens N-1A and N-2A had an approximate ultimate strength of 170,000 psi as documented in Structures Group Report and Boeing document MDC-00K99115.

⁵ Stress ratio is ratio of the minimum stress to the maximum stress.

The fifth sample (N-2B) was pulled in pure tension to fracture without cycling.

The fracture surfaces of all test samples were examined visually and with a scanning electron microscope (SEM) as were the QST fractures.

Results

A numerical summary of the test results is displayed in the following table.

Table A Summary of Test Conditions and Numerical Results								
Specimen	Notes	Diameters	Area	Approx Peak Load	Minimum Load	Peak Stress	Cycles to fracture	Load at fracture
		(inch)	(sq inch)	(pounds)	(Pounds)	(psi)		(lbs)
N-3B	Major Diameter	0.499	0.195565	Test apparatus specimen				
N982AS	Minor Diameter Before	Not measured						
	Minor Diameter After	0.44157	0.15314					
N-1B	Major Diameter	0.498	0.194782					
N982AS	Minor Diameter Before	0.4614	0.167203	23,374	2,337	139,794	1,549	At 23,385
	Minor Diameter After	0.45868	0.165238					
N-1A	Major Diameter	0.500	0.196349					
QST I	Minor Diameter Before	0.45853	0.165132	27,490	2,963	166,473	389	At 27,746
New	Minor Diameter After	0.45332	0.161398					
N-2A	Major Diameter	0.4975	0.194391					
QST I	Minor Diameter Before	0.46185	0.16753	31,102	3,110	185,651	100	At 31,362
New	Minor Diameter After	0.45398	0.161869					
N-2B	Major Diameter	0.4995	0.195957					
N982AS	Minor Diameter Before	0.46055	0.166588	33,198		199,282	1	At 33,198
	Minor Diameter After	0.44004	0.152081					

Examination Summary

Visual examinations found that the three cycled specimens displayed crescent shaped reflective bands on the fracture surfaces similar in overall appearance to the accident torque tube. The reflective bands displayed fatigue striations indicating multiple initiation sites in the root of the first full thread as did the accident torque tube. Outside the bands, the fracture topography was entirely ductile dimples indicative of overstress fracturing away from the fatigue band.

The fracture surfaces of specimens N-3B and N-2B, did not display the crescent reflective band nor did those from the two Quill Shaft Tests. These specimens fractured in the first full thread from one end and all displayed ductile dimple fracture features over the entire area of the separation.

Examinations of each specimen are detailed in the sections below.

Specimen N-3B

Specimen N-3B was the first specimen tested and used to setup the test apparatus. The test setup included a washer with a 10° slope placed under one end of the specimen. The washer was intended to insure off-axis loading of the specimen during the fatigue testing. The specimen was subjected to 25 cycles at each increment of estimate maximum stresses: 100, 120, 130, 140, 150, 160, and 170 ksi⁶. At the maximum stress of 170 ksi, the specimen experienced only one cycle before it failed.

Macroscopic examination revealed fracture traces leading from the first full thread root on one side of the specimen and propagating to the diametrically opposite side. See figure 3. The initial portion of the fracture was flat; however, the entire fracture surface exhibited a dull coarse-grained texture surrounded by a shear lip, typical of an overstress fracture region. The terminal portion of the fracture occurred along an oblique plane. There was no evidence of a band, similar the band found on the ASA 261 quill shaft fracture surface. SEM study confirmed a predominant dimple mode of rupture, indicative of an overstress fracture region. See figure 4.

Specimen N-1B

Specimen N-1B had been subjected to axial fatigue testing with an estimated maximum stress of 140 ksi. The specimen fractured after 1,549 cycles. Macroscopic examination revealed fracture traces leading from the first full thread root on one side of the specimen and propagating to the diametrically opposite side. See figure 5. The fracture surface exhibited a flat, fine-grained textured band (reflective band) surrounding approximately 70% of the outer periphery of the fracture surface. The remaining fracture surface, beyond the flat band, exhibited a dull coarse-grained texture, typical of a ductile overstress separation. A majority of the fracture surface was relatively flat; however, the terminal portion of the fracture surface occurred along an oblique plane. No evidence of a fine-grained texture was observed along the periphery of the terminal, oblique region.

SEM analysis of the reflective band revealed multiple fatigue origins emanating from the thread root. Figure 6 contains SEM images of the reflective band in the central

⁶ Ksi—thousand pounds per square inch. These stress levels were based on the major diameter of the threads. Later stress levels were based on the minor diameter of the threads and would be correspondingly higher.

region of the crescent and to one side. In the central region of the reflective band, fatigue striations were clearly visible emanating from multiple locations in the thread root to a depth of about 0.024 inches. Fatigue striation mixed with ductile dimples extended an additional 0.015 inches for a total band depth of approximately 0.04 inches. The remaining fracture surface beyond the reflective band revealed a predominant dimple mode of rupture, indicative of overstress separation. Figure 7 displays typical fatigue, mixed and overstress fracture features found in the different areas of the separation.

Specimen N-1A

Specimen N-1A had been subjected to axial fatigue testing with an approximate maximum stress of 166 ksi. The specimen failed after 389 cycles. Macroscopic examination revealed fracture traces leading from the first full thread root on one side of the specimen and propagating toward the diametrically opposite side. See figure 8. The fracture surface exhibited a reflective band around approximately 80% of the fracture surface. See lower view of figure 8. The remaining fracture surface, beyond the flat band, exhibited a dull coarse-grained texture, typical of a ductile overstress separation. The terminal portion of the fracture occurred along an oblique plane. No evidence of a fine-grained textured band was found along the periphery of this terminal region.

SEM analysis of the reflective band revealed multiple fatigue origins emanating from the thread root. The band was similar to that seen on specimen N-1B but was much thinner. Figure 9 contains SEM images of the reflective band in the central region of the crescent and to one side. In the central region of the reflective band, fatigue striations were clearly visible emanating from multiple locations in the thread root to a depth of about 0.004 inches. Fatigue striation mixed with ductile dimples extended an additional 0.004 inches for a total band depth of approximately 0.008 inches. The remaining fracture surface beyond the flat band revealed a predominant dimple mode of rupture, indicative of an overstress fracture region. Figure 10 displays typical fatigue, mixed and overstress fracture features found in the different areas of the separation.

Specimen N-2A

Specimen N-2A was subjected to axial fatigue testing with an estimated maximum stress of 185 ksi. The specimen failed at 100 cycles. Macroscopic examination revealed fracture traces leading from the first full thread root on one side of the specimen and propagating toward the diametrically opposite side. See figure 11. The fracture surface exhibited a reflective band surrounding approximately 50% of the outer periphery of the fracture surface. This thin reflective band was similar in overall appearance and shape to the thin band found on specimens N-1B and N-1A. The remaining fracture surface, beyond the flat band, exhibited a dull coarse-grained texture, typical of a ductile overstress separation. A majority of the fracture surface was relatively flat; however, the terminal portion of the fracture surface occurred along an oblique plane. No evidence of a fine-grained texture was observed along the periphery of the terminal, oblique region.

SEM analysis of the reflective band revealed multiple fatigue origins emanating from the thread root. Figure 12 contains SEM images of the reflective band in the central region of the crescent and to one side. Fatigue striations were clearly visible emanating from origin in the thread root to a depth of about 0.004 inches. The fracture features then transformed into entirely ductile dimple with little or no zone of mixed features that were seen in specimens N-1B, and N-1A. The remaining fracture surface beyond the flat band revealed a predominant dimple mode of rupture, indicative of an overstress fracture region. Figure 13 displays typical fatigue and overstress fracture features found in the different areas of the separation.

Specimen N-2B

Specimen N-2B was not cycled but rather loaded to failure in single tension cycle. The specimen separated at approximately 200 ksi. Macroscopic examination revealed fracture traces leading from the first full thread root on one side of the specimen and propagating toward the diametrically opposite side. See figure 14. The initial portion of the fracture surface appeared flat; however, the entire fracture surface exhibited a dull coarse-grained texture, typical of an overstress separation. A small shear lip surrounded the entire fracture surface. The terminal portion of the fracture occurred along an oblique plane. No evidence of a reflective band was found along the outer periphery of the fracture surface. See figure 15.

SEM analysis revealed a predominant dimple mode of rupture, indicative of ductile overstress separation. See Figure 16. No evidence of fatigue striations or other brittle/slow growth mechanism of failure was observed.

Torque Tube Fracture from Quill Shaft Test I

After the completion of the Quill Shaft Test I on July 26, 2000, the fracture surface of the separated torque tube was examined at the Boeing Huntington Beach M&PE laboratories. Macroscopic optical and SEM examinations found fracture traces indicating that the fracture initiated on one side of the tube in the root of the first full thread closest the lower spline region on the torque tube and propagated toward the diametrically opposite side. See figure 17. The fracture surface appeared flat and the entire fracture surface exhibited a dull coarse-grained texture, typical of an overstress separation. The fracture surface did not reveal a reflective band at the outer periphery of the fracture surface but rather a small shear lip was present entirely around the fracture. SEM analysis revealed a ductile dimple mode of rupture, indicative of ductile overstress fracture over the entire separation.

Torque Tube Fracture from Quill Shaft Test II

Macroscopic and SEM analyses revealed that the failure of the torque tube from QST II (October 2, 2000) was very similar to the fracture of the torque tube from Quill Shaft Test I.

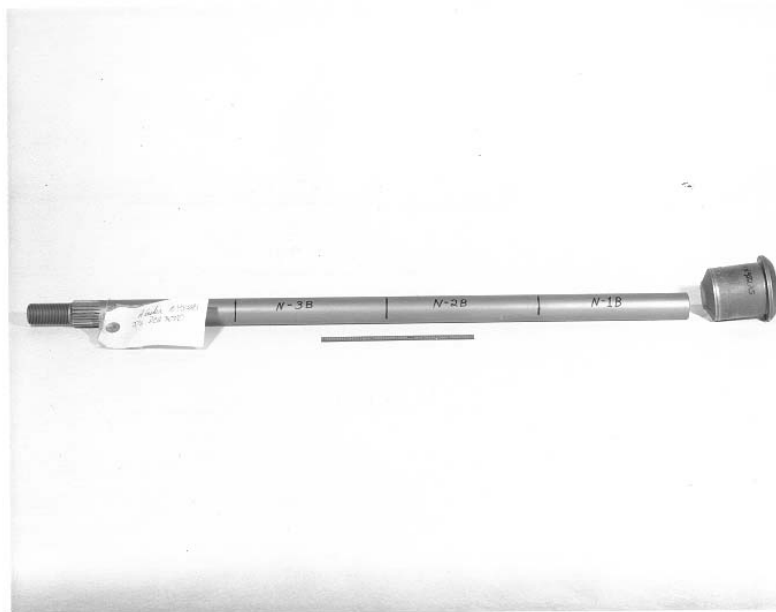
Macroscopic optical and SEM examinations found fracture traces indicating that the fracture initiated on one side of the tube in the root of the first full thread closest the lower spline region on the torque tube and propagated toward the diametrically opposite side. See Figure 18. The entire fracture surface was surrounded with a shear lip and had a dull coarse-grained texture consistent with an overstress separation. The shear lip region at the initiation site was extremely small. SEM analysis revealed a predominant ductile dimple mode of rupture, indicative of overstress separation. There was no evidence of preexisting cracks.

Joe Epperson
Senior Metallurgist



ImageNo:109A0371, Project No:A00253

— 100 mm —



ImageNo: 109A0372, Project No:A00253

— 200 mm —

Figure 1--The test specimens were cut from the new torque tube used in QST I (top) and from the tube removed from N982AS (bottom).

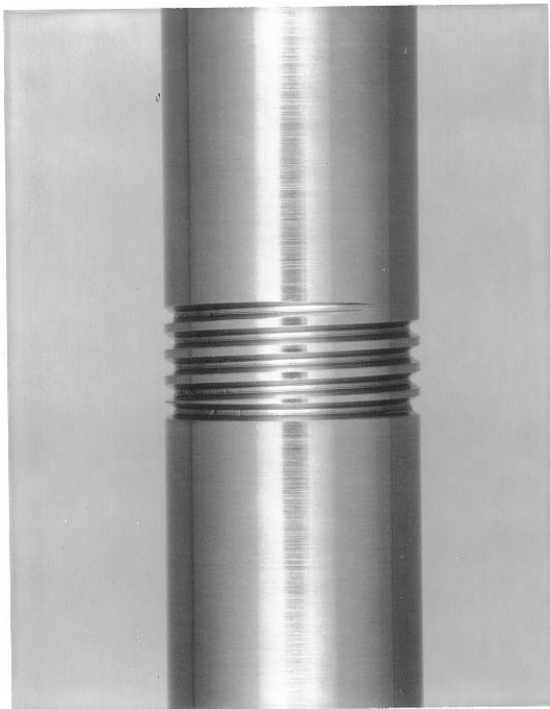
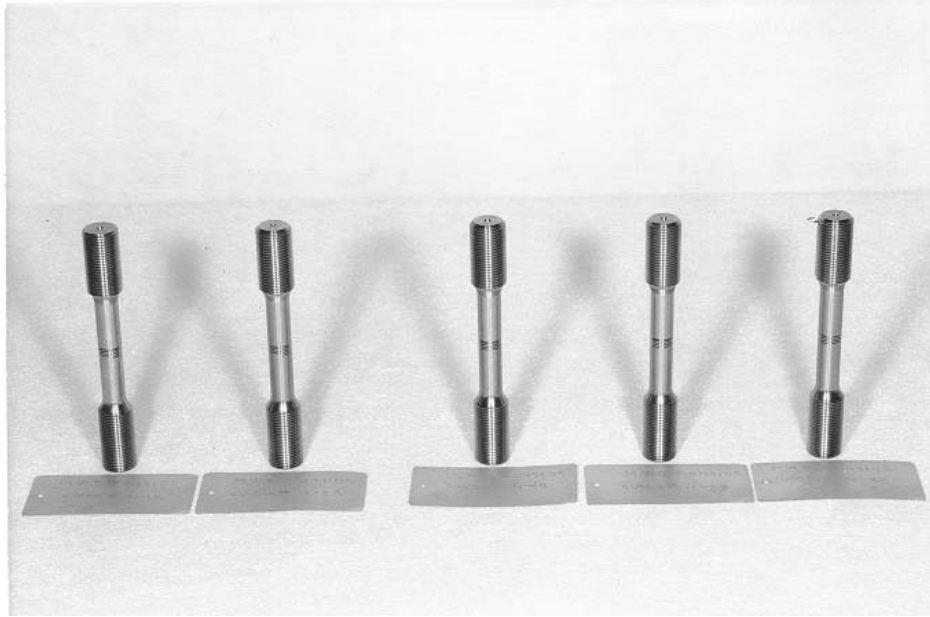


Figure 2--An overall view of the test specimens (top) and a closer view of typical threading in the center of the spemens.

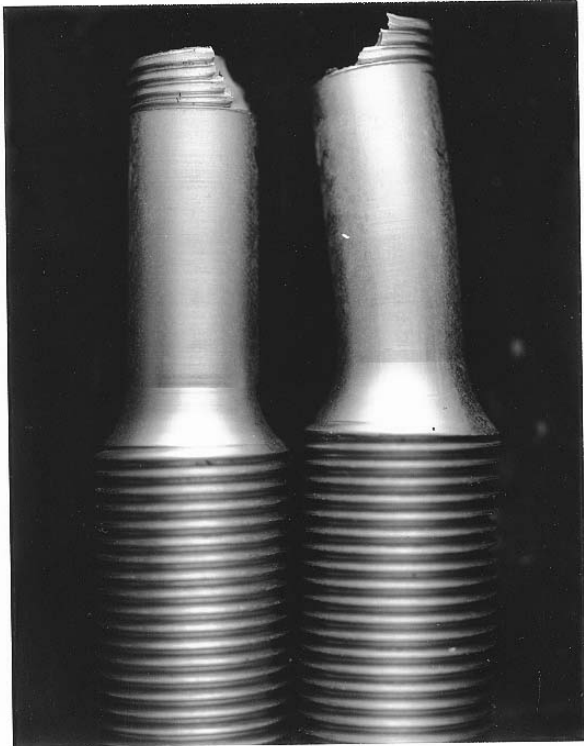
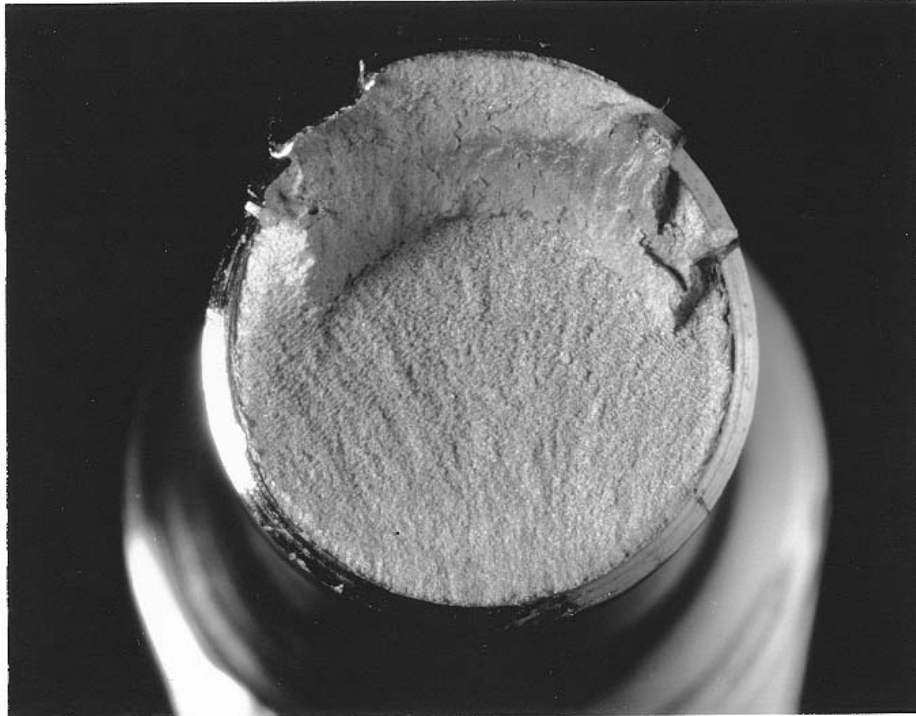


Figure 3--Specimen N-3B after the test. Note the bend in the right half of the specimen. The fracture face (below) was typical of an overstress separation and does not show a reflective band. Fracture initiation was from bottom of fracture as shown below, with the final shear lip at the top.



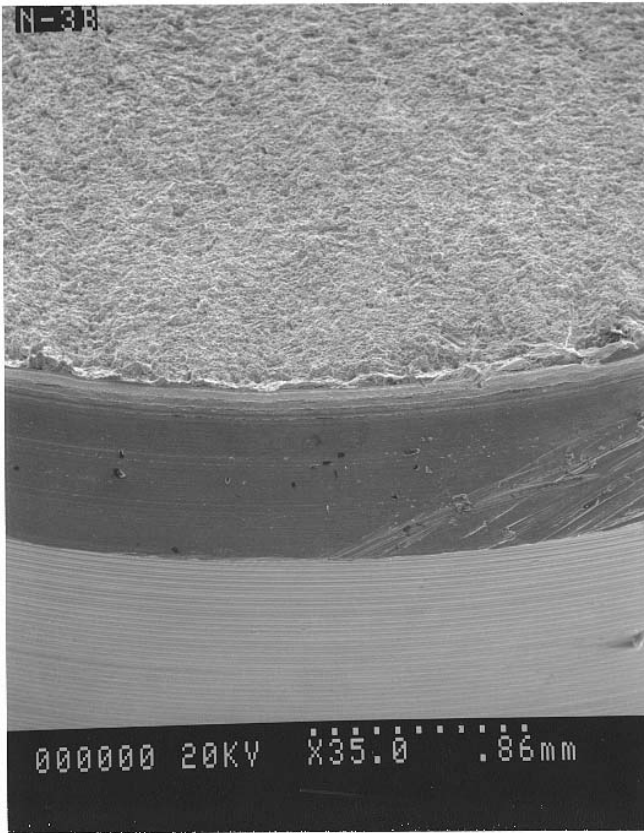
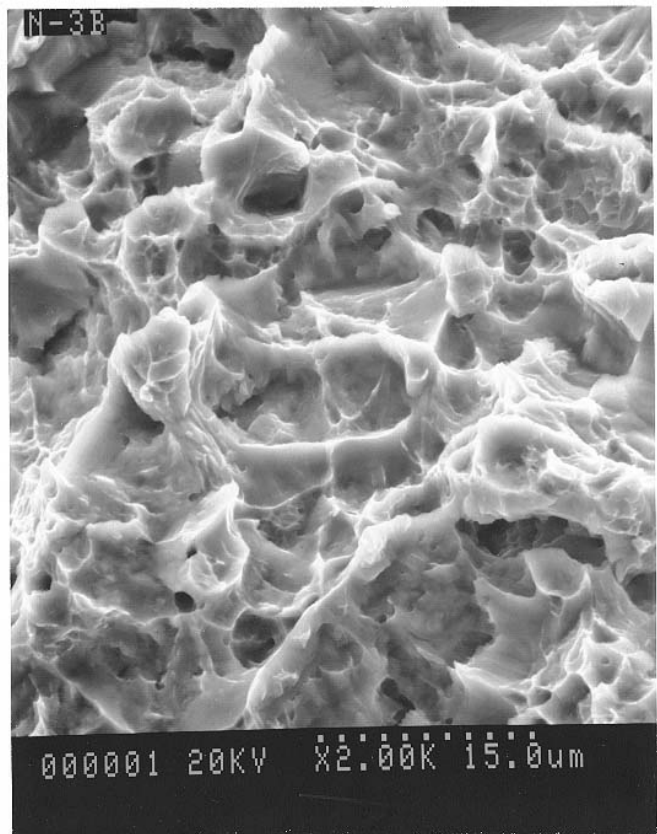


Figure 4--SEM views of specimen N-3B showing ductile overstress fracture features at low and high magnifications.

ImageNo:109A0438, Project No:A00253

┆ 500 μ m ┆



ImageNo: 109A0439, Project No:A00253

┆ 10 μ m ┆

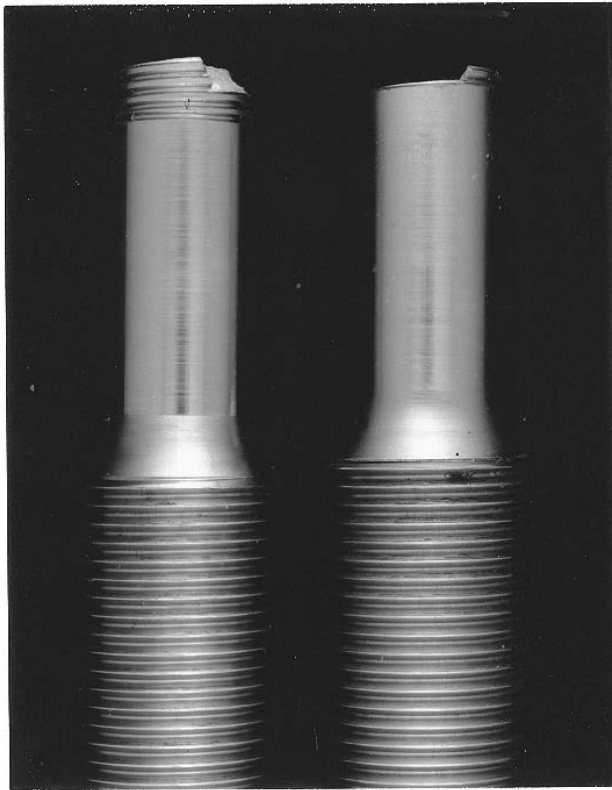
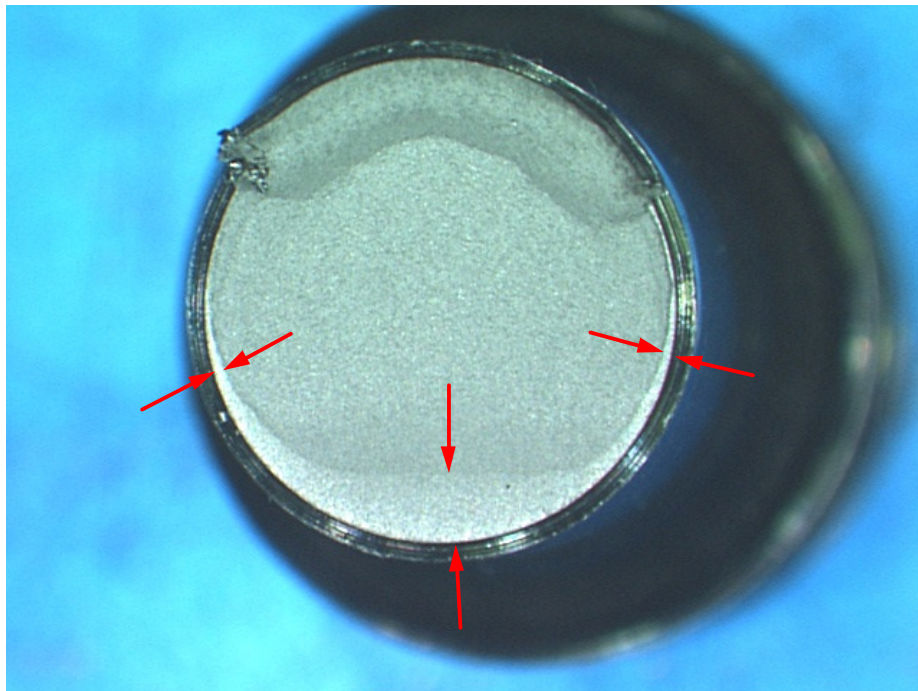
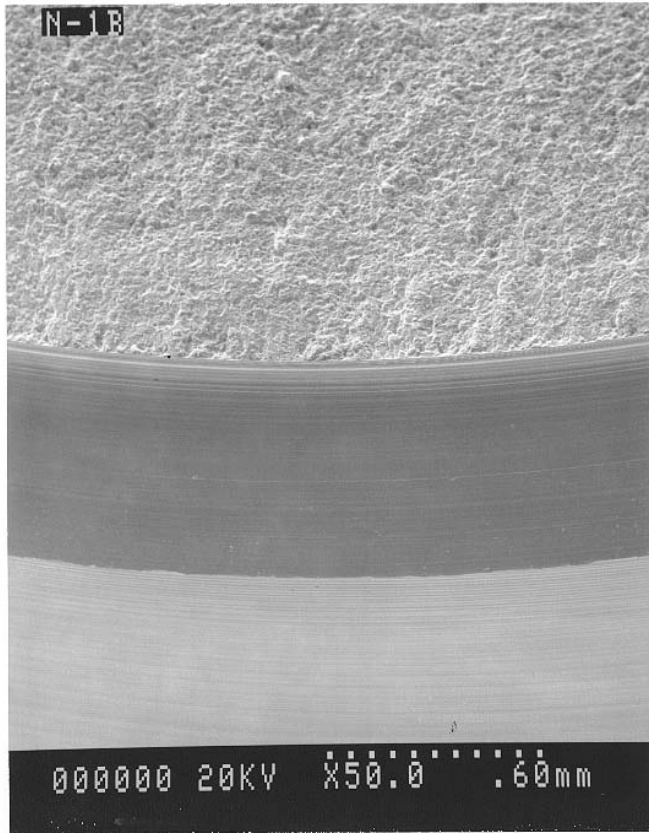


Figure 5--Specimen N-1B after the test. Fracture face (below) shows initiation and reflective band (between arrows) at bottom of view and final shear lip at top.



ImageNo:109A0456 , Project No: A00253

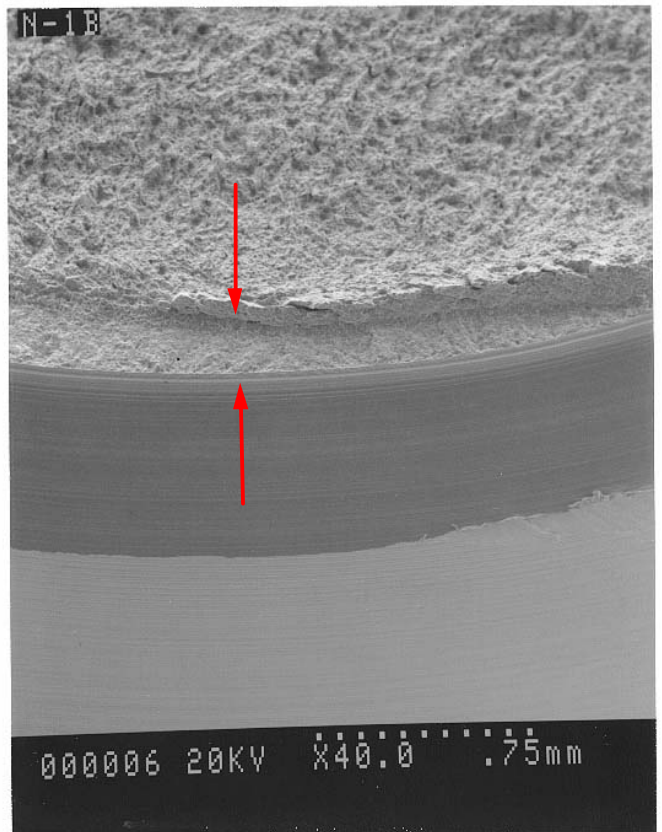
5 mm



ImageNo:109A0432, Project No:A00253

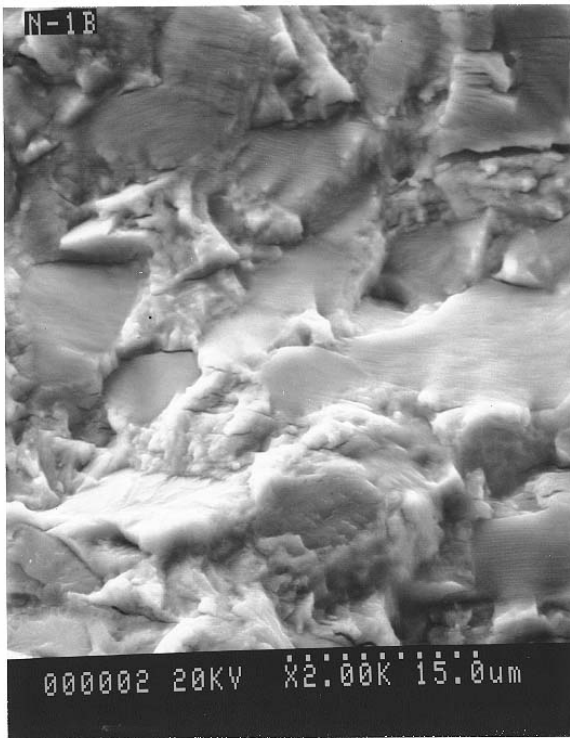
— 500 μ m —

Figure 6--Two SEM views of the fracture surface of specimen N-1B showing the origin area at left and a view of the side portion of the band below. The reflective band is clearly visible in the lower view.

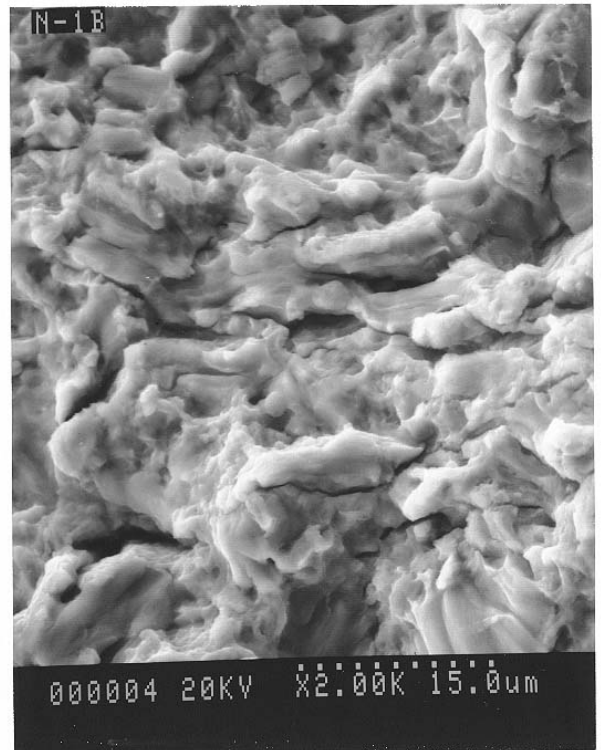


ImageNo: 109A0433, Project No:A00253

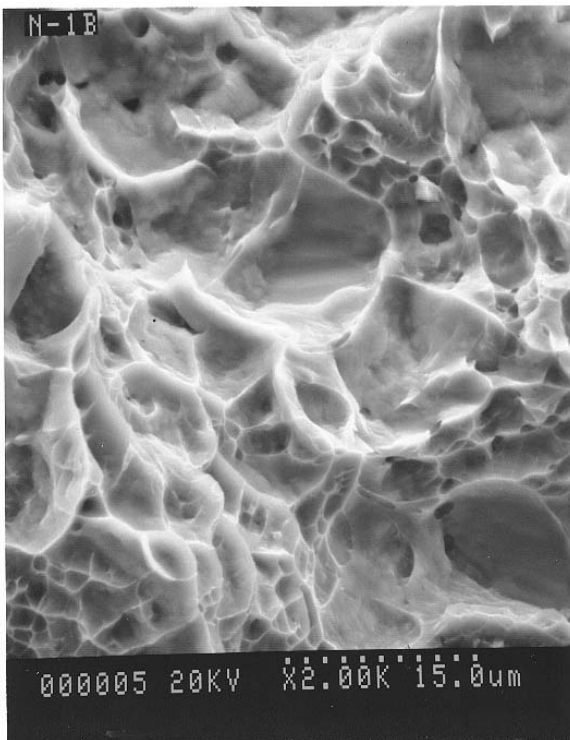
— 500 μ m —



ImageNo:109A0434, Project No:A00253 | 10 μm |



ImageNo: 109A0436, Project No:A00253 | 10 μm |



ImageNo:@ImageNo/1@, Project No:A00253 | 10 μm |

Figure 7--Three SEM views of the fracture face of specimen N-1B. Upper left shows fatigue striations within the reflective band near the initiation area. Upper right show the region of mixed striations and dimples near the terminus of the reflective band. View at lower left shows the dimples typical on the remaining fracture area.

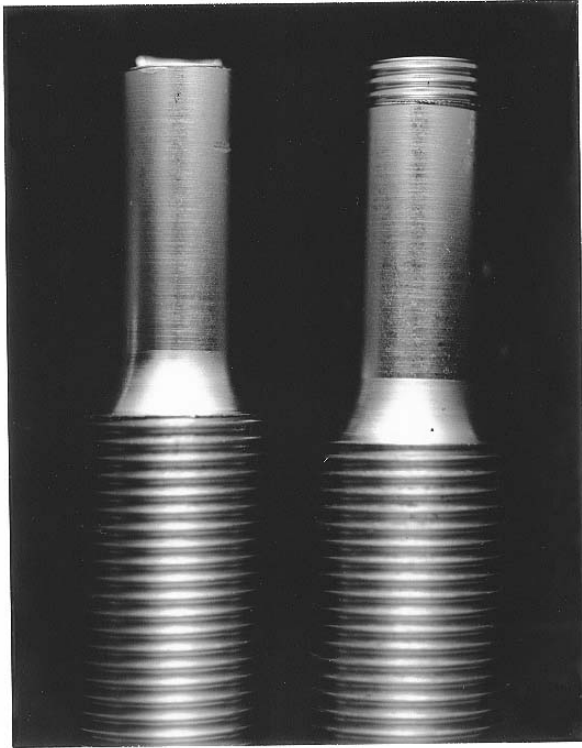
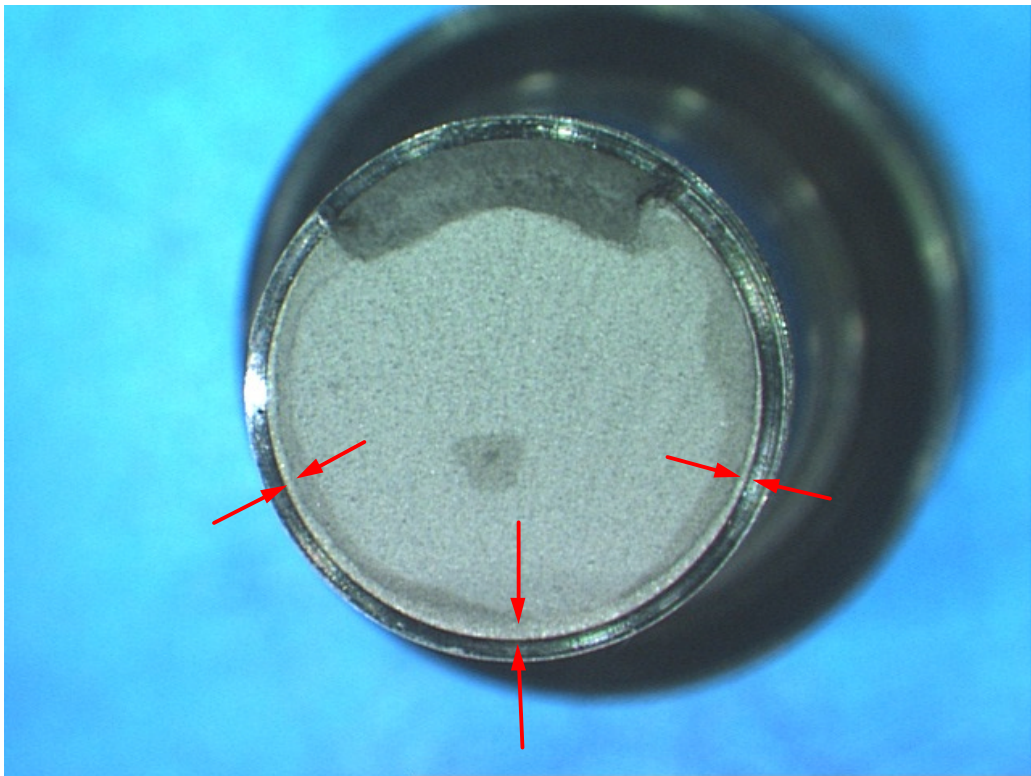
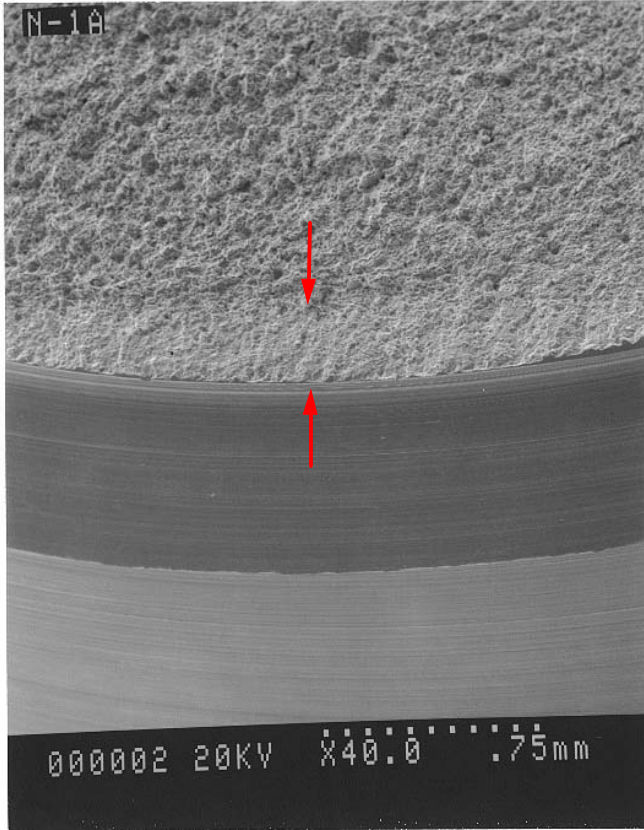


Figure 8--Specimen N-1A after the test. Fracture face (below) shows initiation and reflective band (between arrows) at bottom of view and final shear lip at top.

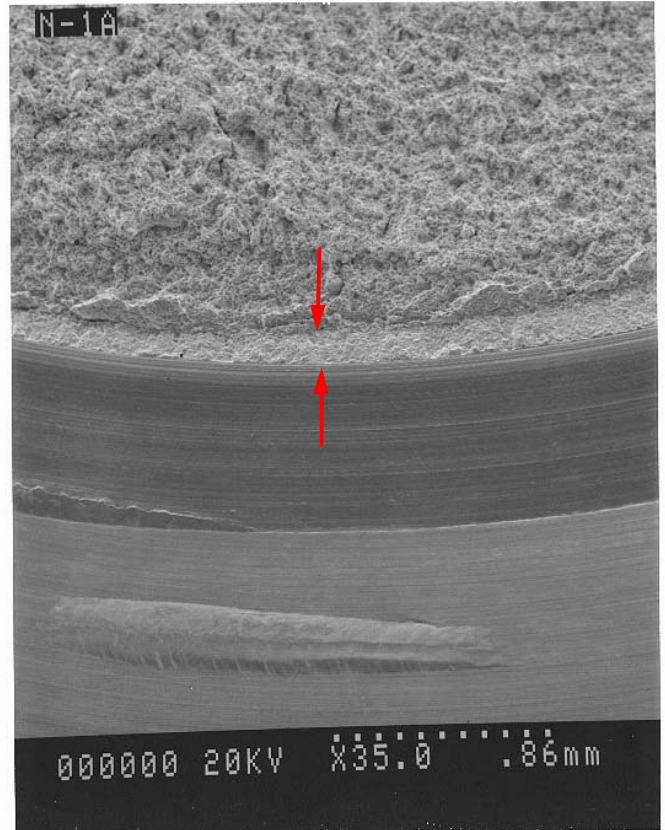


ImageNo:109A0458 , Project No: A00253



ImageNo:109A0420, Project No:A00253

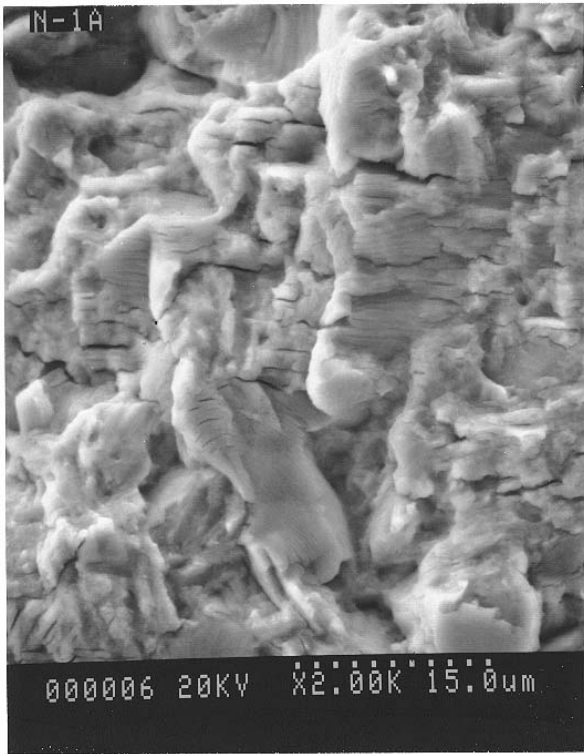
┌ 500 μm ─┘



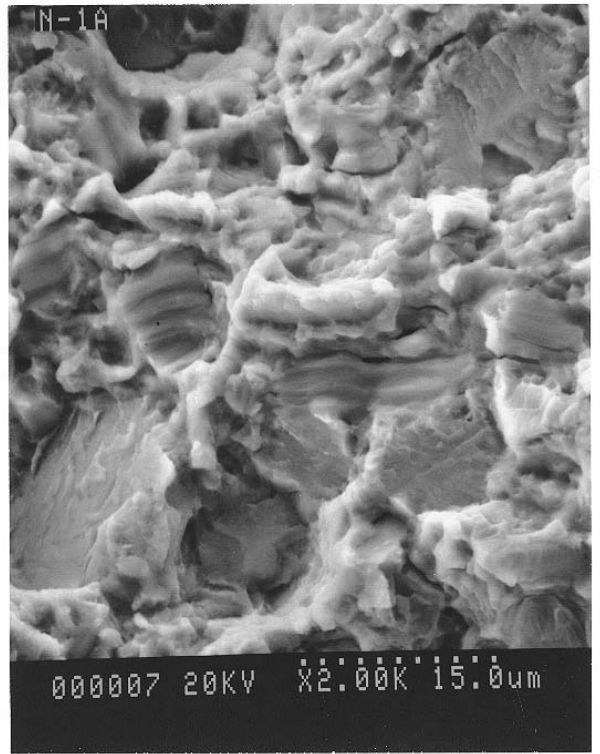
ImageNo: 109A0421, Project No:A00253

┌ 500 μm ─┘

Figure 9--Two SEM views showing the reflective band (between arrows) in the initiation area (left) and around the side of the specimen (right). Specimen N-1A



ImageNo:109A0422, Project No:A00253 | 10 µm |



ImageNo: 109A0423, Project No:A00253 | 10 µm |

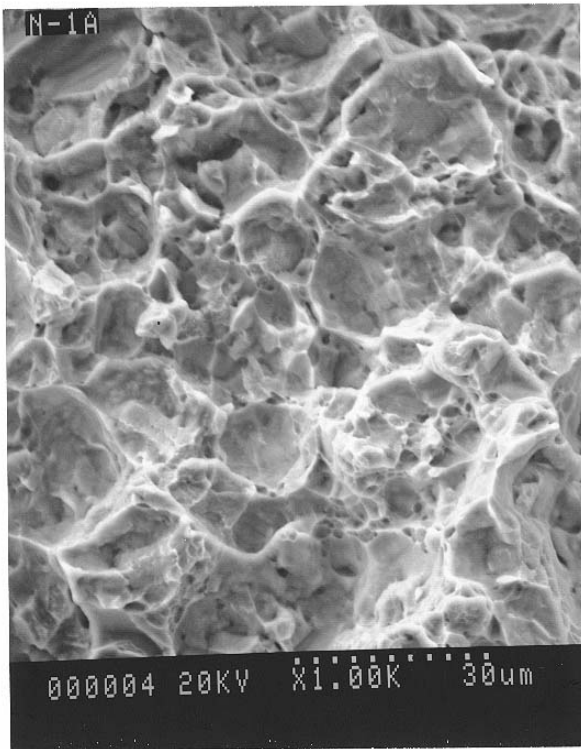


Figure 10--Three SEM views of the fracture face of specimen N-1A. Upper left shows fatigue striations within the reflective band near the initiation area. Upper right shows the region of mixed striations and dimples near the terminus of the reflective band. View at lower left shows the dimples typical on the remaining fracture area.

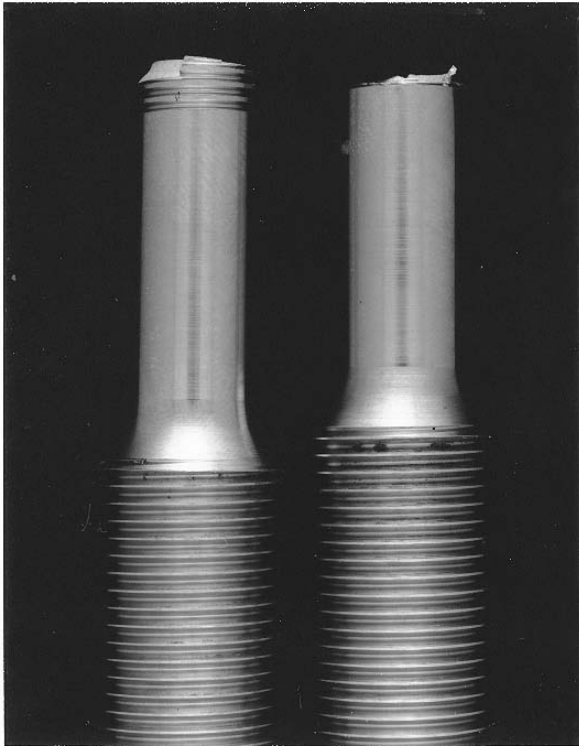
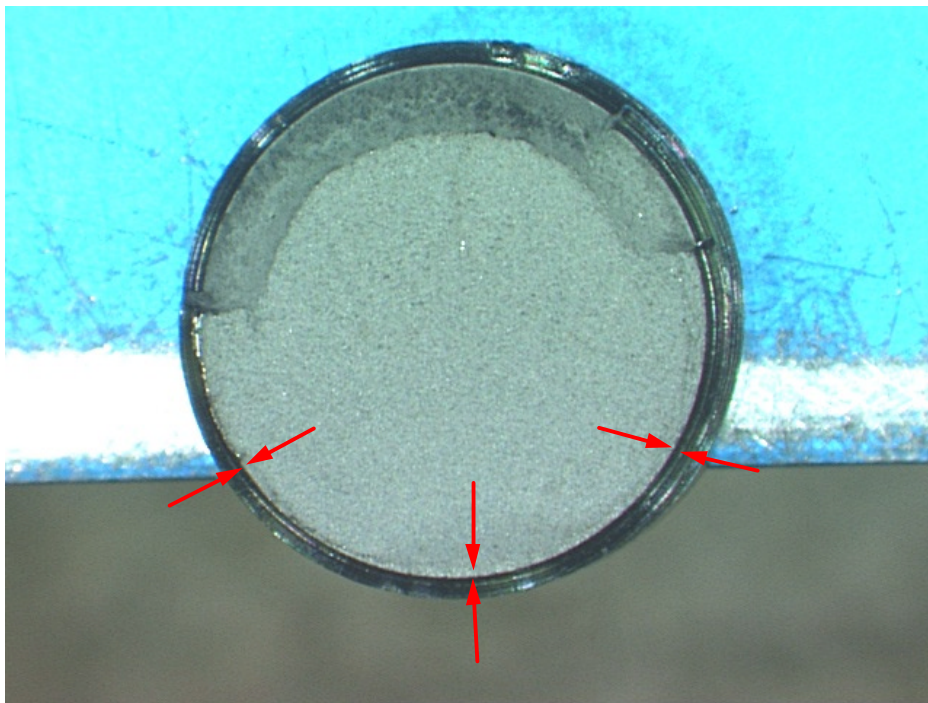
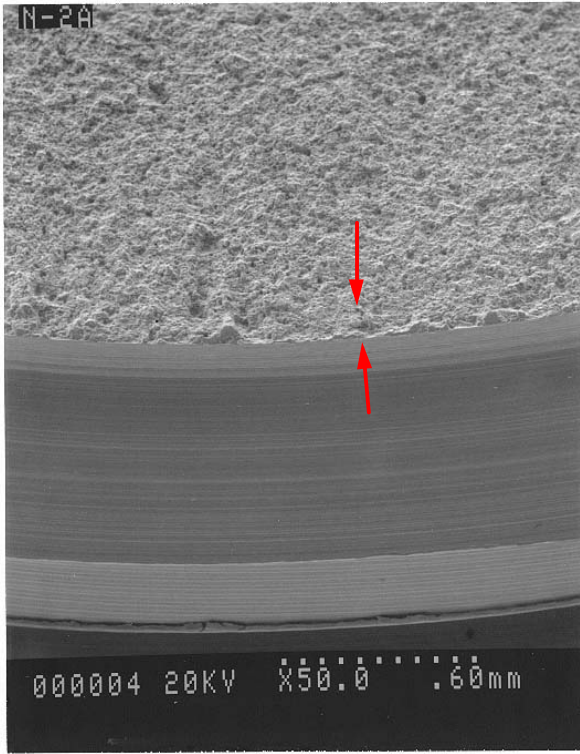


Figure 11--Specimen N-2A after the test. Fracture face (below) shows initiation and reflective band (between arrows) at bottom of view and final shear lip at top.



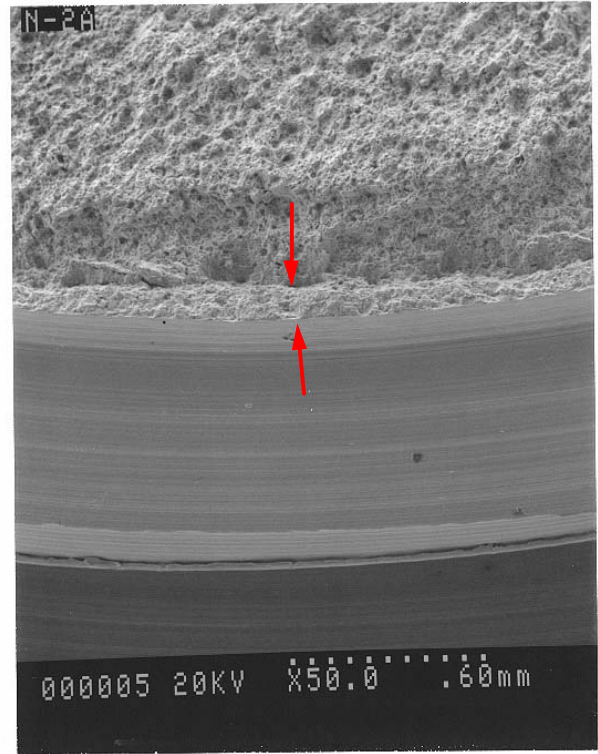
ImageNo:109A0460 , Project No: A00253

5 mm



ImageNo:109A0425, Project No:A00253

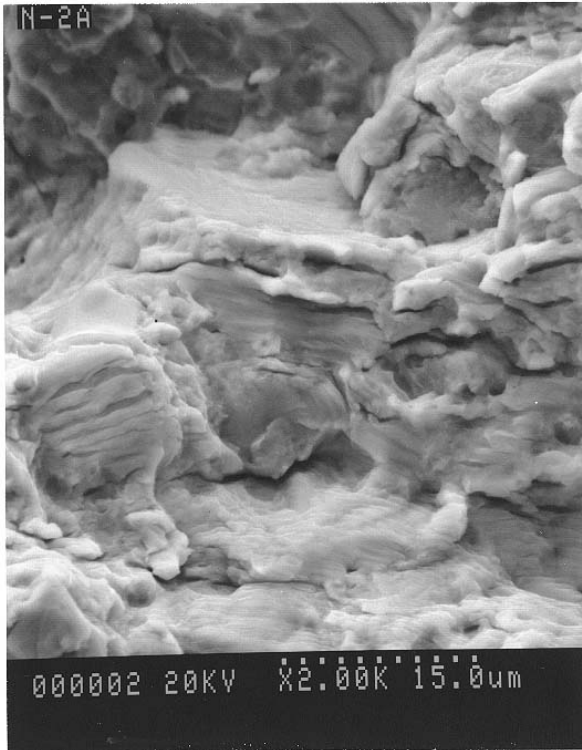
— 500 μ m —



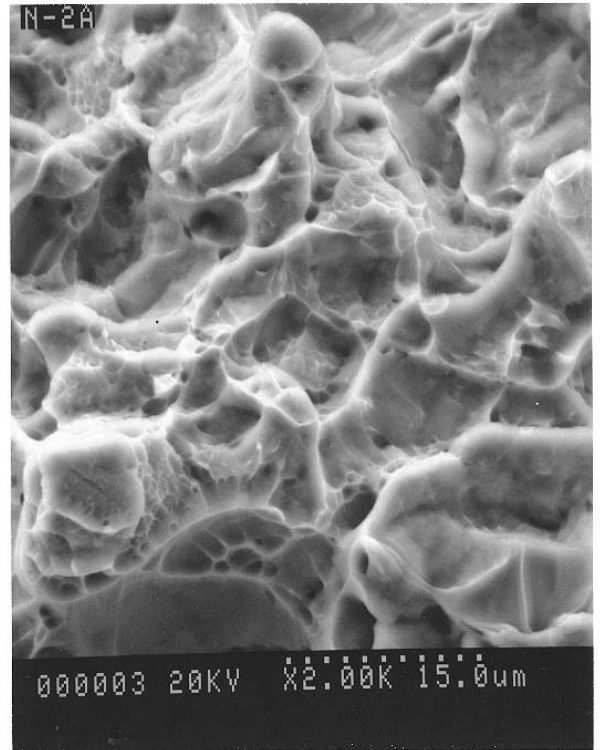
ImageNo: 109A0426, Project No:A00253

— 500 μ m —

Figure 12--Two SEM views showing the reflective band (between arrows) in the initiation area (left) and around the side of the specimen (right).



ImageNo:109A0427, Project No:A00253 ┆ 10 μ m ┆



ImageNo: 109A0428, Project No:A00253 ┆ 10 μ m ┆

Figure 13--Two SEM views of the fracture face of specimen N-2A. View at left shows typical striations in the reflective band near the origin. Right view shows typical ductile dimples on remainder of fracture.

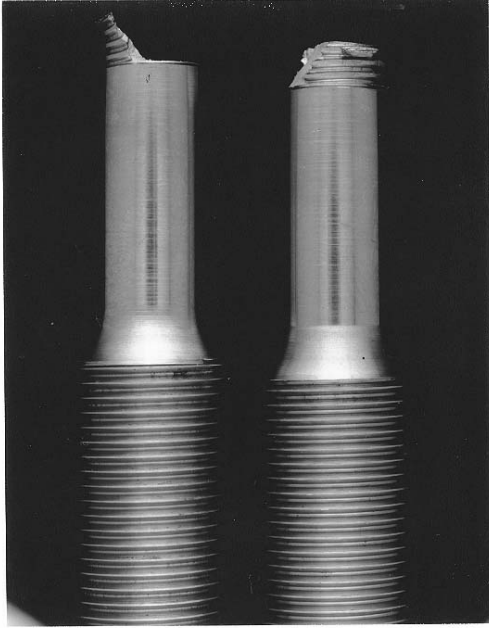
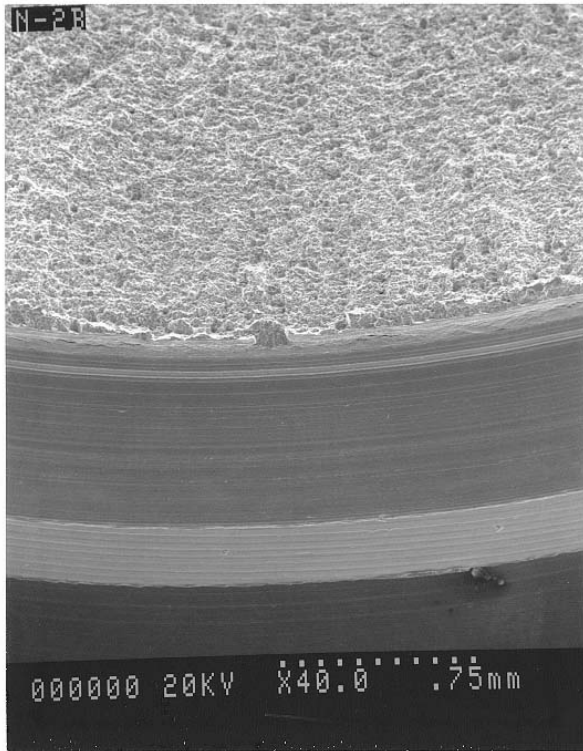
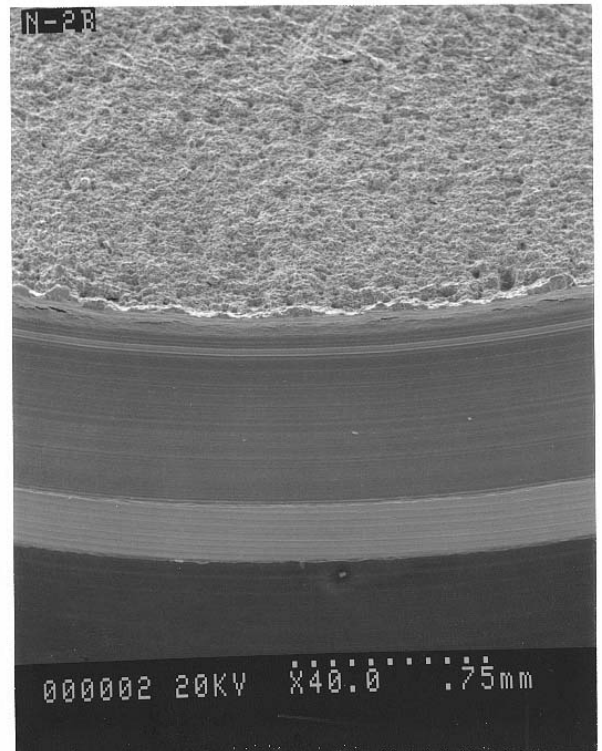


Figure 14--Specimen N-2B after the tensioning to fracture. Fracture face (below) shows initiation at bottom of view and final shear lip at top.



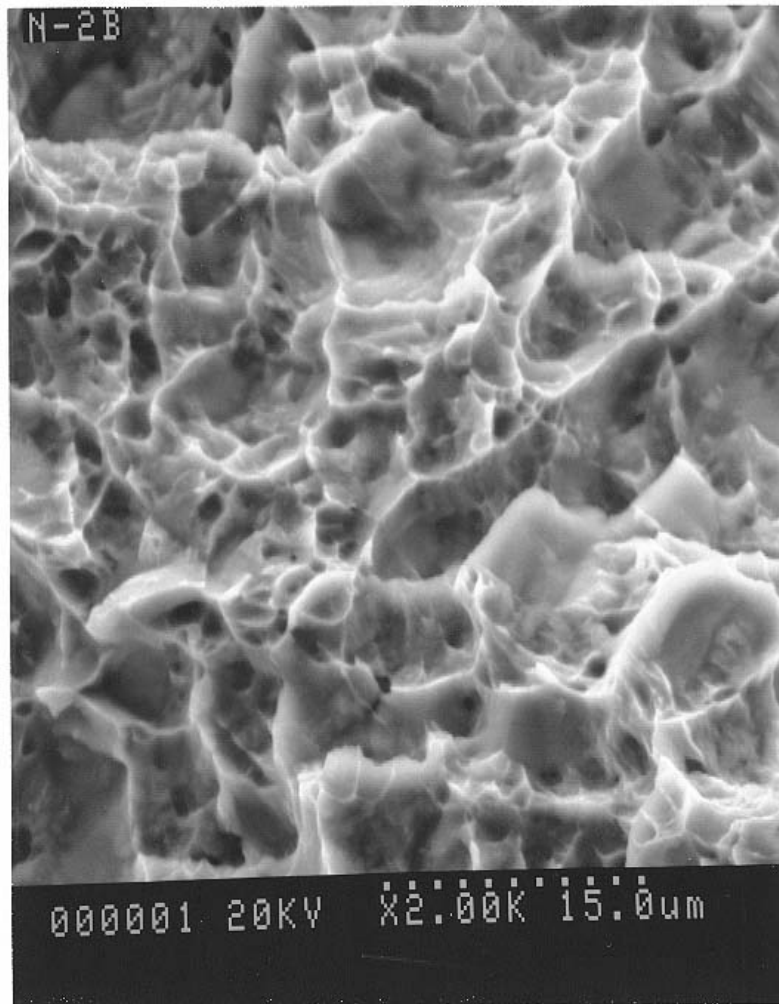


ImageNo:109A0429, Project No:A00253 | 500 μm |



ImageNo: 109A0430, Project No:A00253 | 500 μm |

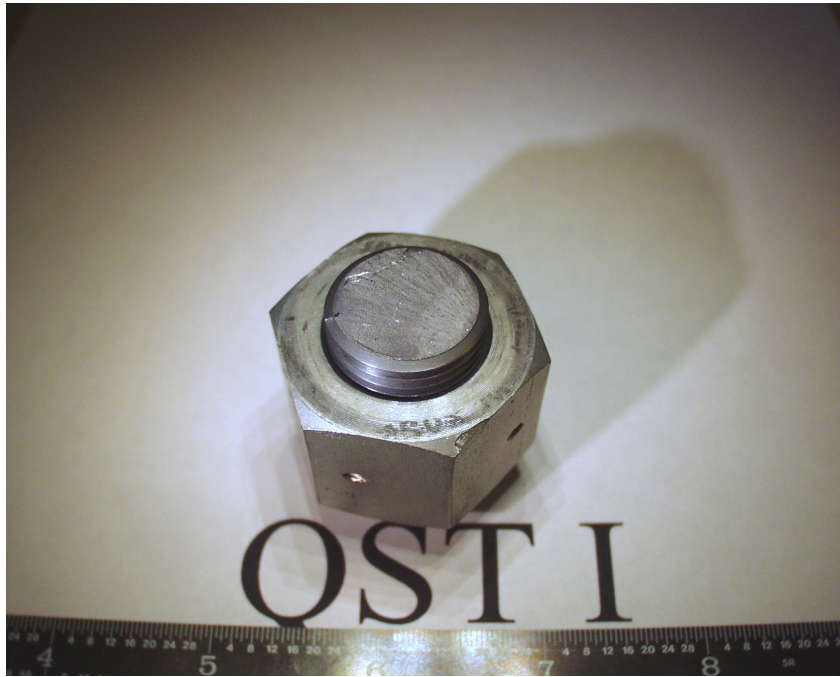
Figure 15--Two SEM views showing the lack of a reflective band on the specimen. Fracture initiation area at left and the side of the specimen at right.



ImageNo:109A0431, Project No:A00253

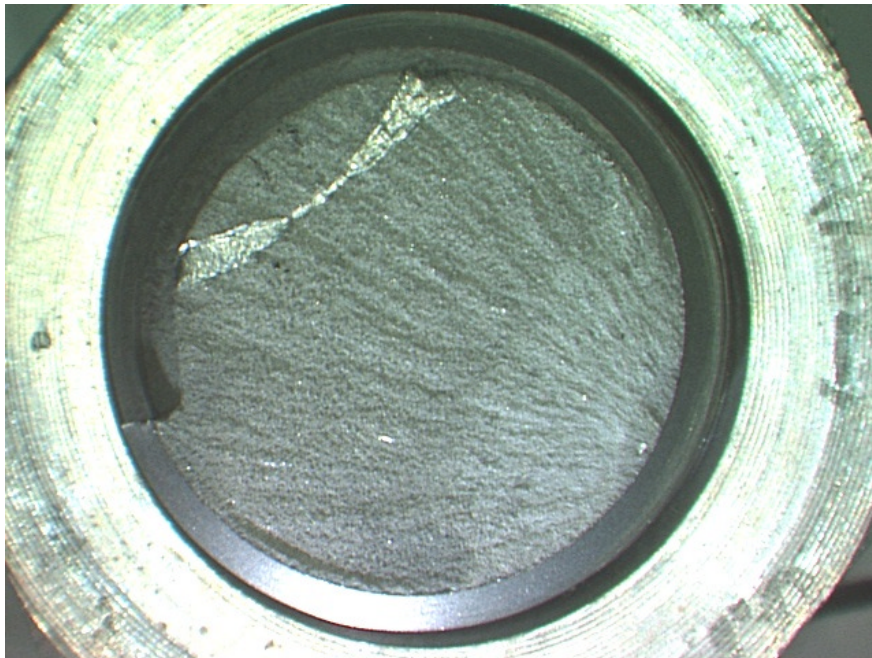
— 10 μ m —

Figure 16--Typical ductile dimple found on the entire fracture face of specimen N-2B.



ImageNo:109A0468, Project No:A00253

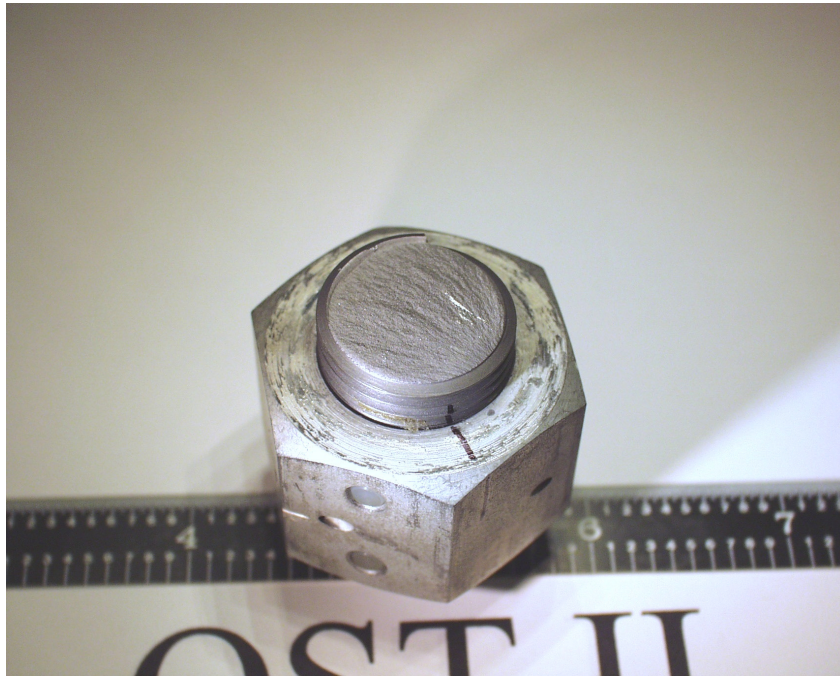
| 20 mm |



ImageNo: 109A0466, Project No:A00253

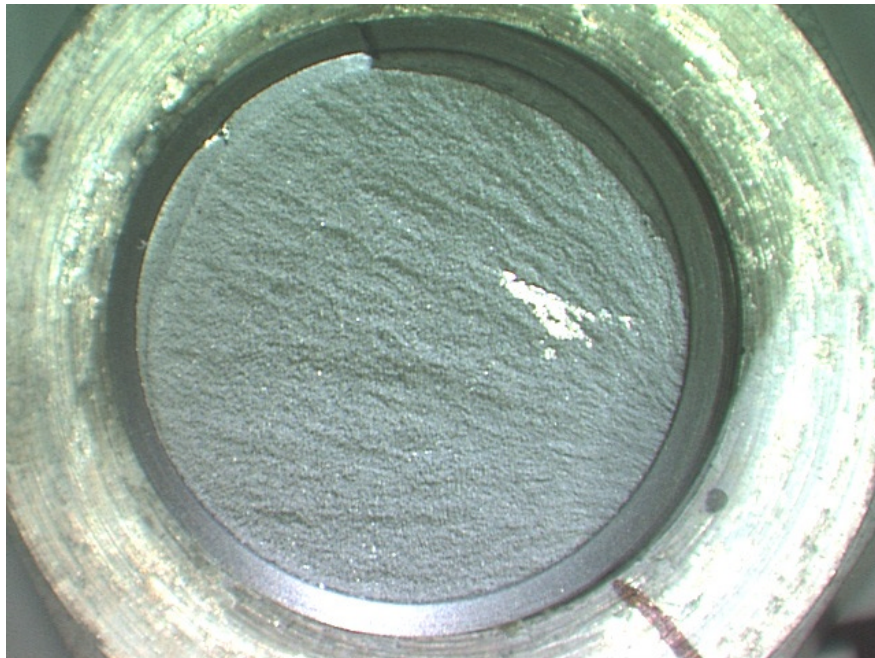
| 10 mm |

Figure 17--Two view of the fractured torque tube from QST I. Fracture initiated in lower right quadrant (lower view) and diametrically propagated across the tube. No reflective band was found.



ImageNo:109A0467, Project No:A00253

— 20 mm —



ImageNo: 109A0463, Project No:A00253

— 10 mm —

Figure 18--Two view of the fractured torque tube from QST II. Fracture initiated in lower right quadrant (lower view) and diametrically propagated across the tube. No reflective band was found.